Lawrence Berkeley National Laboratory

LBL Publications

Title

Improving LMOF luminescence quantum yield through guest-mediated rigidification

Permalink

https://escholarship.org/uc/item/5z89676f

Journal

Journal of Materials Chemistry C, 7(46)

ISSN

2050-7526

Authors

Lustig, William P

Teat, Simon J

Li, Jing

Publication Date

2019-11-28

DOI

10.1039/c9tc05216j

Peer reviewed

eScholarship.org Powered by the California Digital Library
University of California

Improving LMOF Luminescence Quantum Yield through Guest-Mediated Rigidification

William P. Lustig,[a] Simon J. Teat,[b] and Jing Li*,[a]

Luminescent metal-organic frameworks (LMOFs) are among the fastest growing solid-state optical materials and have been studied for a wide variety of applications. However, when developing a new LMOF, it can be challenging to balance a strong luminescent quantum yield with all other important properties required by the intended application (appropriate excitation/ emission wavelengths, chemical and physical stability, low toxicity, etc). Being able to post-synthetically improve a LMOF's quantum yield is valuable, as it offers additional tunability in materials design and modification. As framework flexibility can limit quantum yield, post-synthetic methods of rigidifying an LMOF have the potential to improve its performance. This paper discusses a pair of nearly identical isoreticular LMOFs, and uses them as a model system to investigate how framework flexibility affects quantum yield. Introducing optically-inactive guests into a LMOF pore is shown to be effective method of rigidifying the framework, improving the quantum yield of a flexible LMOF from 12.2% to 59.3%—an improvement of nearly 400%.

Introduction

Luminescent metal-organic frameworks (LMOFs) are a rapidly expanding class of photoluminescent solid-state materials composed of metal ions or metal clusters linked into a crystalline, typically porous framework by organic ligand molecules. Luminescence in these materials can arise from a variety of mechanisms and is extremely tunable, which makes LMOFs attractive for a wide variety of applications including use as phosphor materials, optical sensors, imaging agents, and dyes.[1-9] It is extremely important for many of these applications for the LMOF to have strong emission properties, so a significant amount of research has been focused on producing LMOFs with exceptional quantum yields;[10-15] however, it can be challenging to develop an LMOF that possesses both the chemical stability and emission profile required by a given application and a high quantum yield. Post-synthetic strategies for boosting quantum yield are therefore of great interest.

In LMOFs, quantum yields can often be depressed by framework flexibility.[16, 17] Upon excitation, vibrational and rotational modes of the ligands in these structures are often available to return the excited electron to the ground state in a non-radiative fashion. This can be addressed using rigidification strategies first developed for improving quantum yield in flexible organic chromophore molecules; for example, ligand design can be altered to increase rigidity.[18-20] However, solutions like this typically place a design limit on the types of LMOFs which can be used in applications requiring strong photoluminescence. In situations where these strategies cannot work, it is necessary to develop post-synthetic methods for rigidifying the frameworks. One way that this can be accomplished is through "guest-packing", in which loading the porous LMOF with a guest molecule serves to prevent certain vibrational or rotational modes of ligands from being available, and thus enhancing or turning-on luminescence.[16]

In this work, we report the synthesis and structure of [Zn_2(tcbpe)(bpy) or LMOF-263; H_4tcbpe = 1,1,2,2-tetrakis(4-(4-carboxy-phenyl)phenyl)ethene, bpy = 4,4'-bipyridine] and its framework rigidification by a post-synthesis guest-packing approach. For comparison purpose, a previously-reported isoreticular LMOF, [Zn2(tcbpe-F)(bpy) or LMOF-301; H_4tcbpe-F = 1,1,2,2-tetrakis(4-(4-carboxy-3-fluoro-phenyl)phenyl)ethene] is also included in the study.[21] The two LMOFs possess nearly identical ligands, with the only difference being the R group in [Zn2(tcbpe-R)(bpy), which is H in LMOF-263 and F in LMOF-301. This difference permits rotation of a pyridyl

moiety in a neighbouring bpy ligand in LMOF-236, while the rotation is sterically prevented in LMOF-301. These two LMOFs serve as an ideal model system for testing a guest-packing rigidification effect. Guest molecules with various functional groups and of various shapes and sizes are loaded into these two LMOFs, and it is determined that quantum yield is significantly improved in the rotation-allowed LMOF-236 upon loading with n-pentane, as it rigidifies the framework by inducing a framework shift that brings the rotating bpy moiety into contact with the neighbouring framework.

Experimental

Materials.

The ligands H_4tcbpe and H_4tcbpe-F were synthesized according to previously published reports.[11, 21] All solvents, reagents, and catalysts used in the synthesis of these two ligands were purchased from Sigma Aldrich and used without further purification. The ligand bpy, $Zn(NO_3)_2 \cdot 6H_2O$, $Zn(ClO_4)_2 \cdot 6H_2O$ dimethylacetamide (DMA), and HBF_4 used in the synthesis of the LMOFs 236 and 301, as well as all solvents used in the solvent exchange/guest packing experiment, were also purchased from Sigma Aldrich and used without further purification.

Synthesis of LMOFs.

To synthesize LMOF-236, 0.050 mmol $Zn_2(NO_3)_2 \cdot 6H_2O$ was added to 0.025 mmol H_4tcbpe and 0.050 mmol bpy in a glass vial. 4 mL DMA was added, followed by 2 drops of HBF_4, and the solution was sonicated until clear. The vial was sealed and placed in a 100 °C oven for 72 hours, after which the crystals were recovered via filtration. LMOF-301 was synthesized using the reported method.[21]

Solvent exchange.

Solvent exchange was achieved by immersing the LMOF samples in 20 mL of the exchange solvent, and replacing the solvent five times over the course of 10 hours. Solvent was exchanged with a pipet, and without filtering. The samples were then left immersed in the exchange solvent for at least another 24 hours, and stored in the exchange solvent until analysis. Outgassed samples of LMOF-236 and LMOF-301 were prepared by placing the pentane-exchanged samples in a vacuum oven at 40 °C overnight.

Single crystal structure determination.

Single crystal diffraction data for LMOF-236 were collected at 100 K on a Bruker PHOTON100 CMOS diffractometer using the synchrotron source (I = 0.7749 Å) at the Advanced Light Source 11.3.1 Chemical Crystallography beamline, Berkeley National Lab. All non-hydrogen atoms were refined anisotropically. Hydrogen atoms were placed geometrically, constrained, and refined with a riding model. The unresolvable electron density from the framework's void space was removed by SQUEEZE (Table S1, ESI†).

Powder X-ray diffraction (PXRD) analysis.

All powder X-ray diffraction (PXRD) data was collected on a Rigaku Ultima IV diffractometer with a wavelength of 1.5406 Å, scanning from 3° to 35° 2θ at a rate of 2° 2θ/min and with and a step size of 0.2° 2θ.

Thermogravimetric analysis (TGA).

All thermogravimetric analysis data was collected using a TA Instruments Q5000 TGA. Samples were loaded into a Pt pan and heated under a constant dry N2 flow of 20 mL/min. The temperature was gradually increased from ambient to 600 °C at a constant rate of 10 °C/min.

Photoluminescence experiments.

All photoluminescence emission and excitation spectra were collected in the solid state using a Varian Cary Eclipse spectrophotometer at room temperature. Internal quantum yield was measured in the solid state at room temperature for all samples, using a Hamamatsu Quantarus-QY spectrophotometer with a 150 W Xenon monochromatic light source and integrating sphere.

Density functional theory (DFT) calculations.

Density functional theory (DFT) calculations were performed using Gaussian 09, with the B3LYP3 hybrid functional and 6-311++(3df,3pd) basis set.[22-26] The geometries of bpy, H_4tcbpe, and H_4tcbpe-F were optimized, and a frequency calculation was performed after the geometry optimization to confirm that all calculations resulted in a true minimum.

Results and Discussion

LMOF-236 and LMOF-301 structure

LMOF-236 is triclinic and crystallizes in the space group P-1. It is composed of 2D layers of the tcbpe ligand, with each ligand linked to four more through classic zinc-paddlewheel SBUs to form a sheet in the *bc* plane. The pillaring bpy ligand links these sheets into a three dimensional framework by bonding to the axial SBU position in neighbouring layers. Two of these frameworks interpenetrate to give the complete structure (Fig. 1). LMOF-301 is nearly identical to LMOF-236, with the primary difference being the presence of a fluorine atom on the ligand carbon vicinal to the carboxylate group instead of a hydrogen atom.

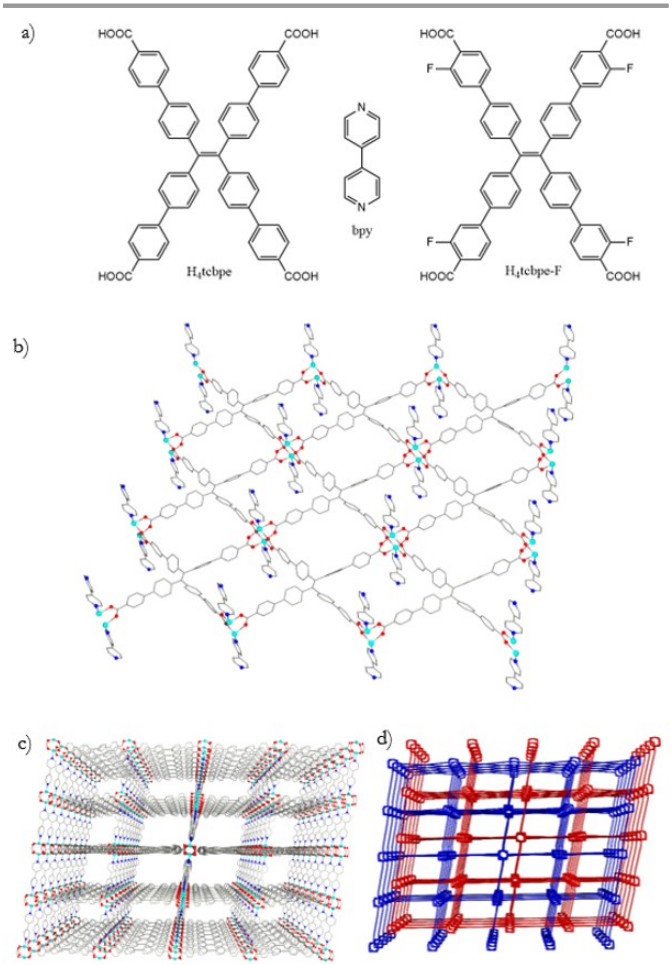

Figure 1. (a) Structures of the ligands H_4tcbpe, bpy, and H_4tcbpe-F (b) 2D sheet of tcbpe ligands in the bc plane linked by zinc paddlewheel SBUs, showing pillaring bpy ligands extending above and below the sheet. (c) Single 3D net of LMOF-236. (d) Schematic of two interpenetrated nets (red and blue), giving the final structure of LMOF-236.

In the structure of LMOF-236, one of the two pyridyl rings in the ligand bpy has a large degree of rotational freedom (Fig. 2). At its closest, the H-H distance between this pyridine group's hydrogen and the closest atom on the neighbouring framework—a hydrogen located on the tcbpe ligand—is 3.8 Å measuring from nucleus to nucleus, which is sufficient to permit free rotation of the pyridine moiety. In fact, the only significant steric interaction is the H-H interaction between pyridyl rings within the same bpy ligand. However, given the exceptionally low thermal barrier to rotation in non-substituted biphenyls at room temperature,[27] it is reasonable to consider this interaction trivial.

The same is not true for LMOF-301, in which the presence of fluorine on the tcbpe-F ligand plays a major role in

(a)

preventing free rotation of the bpy pyridyl ring (Fig. 2). In LMOF-301, the distance between the pyridyl hydrogen and fluorine on the neighbouring framework is just 2.54 Å, suggesting the formation of a weak H-F interaction,[28] and preventing rotation of the pyridyl ring, as continued rotating would further decrease the H-F distance. This is consistent with the single crystal data for LMOFs 236 and 301, as the pyridyl ring in the structure of LMOF-301 shows no disorder, while the same pyridyl ring in LMOF-236 shows significant rotational disorder, even when cooled to 100 K.

Guest-mediated rigidification

The luminescence properties of the chromophoric ligands in LMOF-236 (tcbpe) and LMOF-301 (tcbpe-F) are very similar,[29] as both ligands have nearly identical HOMO-LUMO energy gaps. And although a second ligand (bpy) is present within the structure, it is expected to have minimal effect on the excitation and emission transitions, as DFT calculations indicated that bpy's LUMO is located significantly higher than that of H_4tcbpe and H_4tcbpe-F, while its HOMO is lower than those of the chromophore ligands (Table 1).

Table 1. Calculated LUMO and HOMO energy levels for the ligands bpy, H_4tcbpe, and H_4tcbpe-F.

Ligand	LUMO	HOMO
bpy	-2.02 eV	-7.39 eV
H_4tcbpe	-2.46 eV	-5.87 eV
H_4tcbpe-F	-2.68 eV	-6.10 eV

Both LMOF-263 and LMOF-301 emit at approximately 520 nm when excited by 455 nm light (Fig. S1). For LMOF-301, the quantum yield is fairly consistent regardless of the solvation state of the LMOF, dropping from 50.9% in the as-made state (DMA-solvated) to 45.1% upon solvent removal under 455 nm excitation (Table 2). This performance is consistent with ligand-centered emission from the free chromophoric ligand H_4tcbpe-F, which has a quantum yield of 46.5% under the same excitation conditions (table S2).[29] For LMOF-263, the quantum yield shows a much stronger dependence on the presence of guest molecules within the pore, with the as-made (DMA-solvated) sample's quantum yield under 455 nm excitation of 42.5% dropping to just 12.2% upon removal of the solvent (Table 2). Both of these values are significantly lower than the

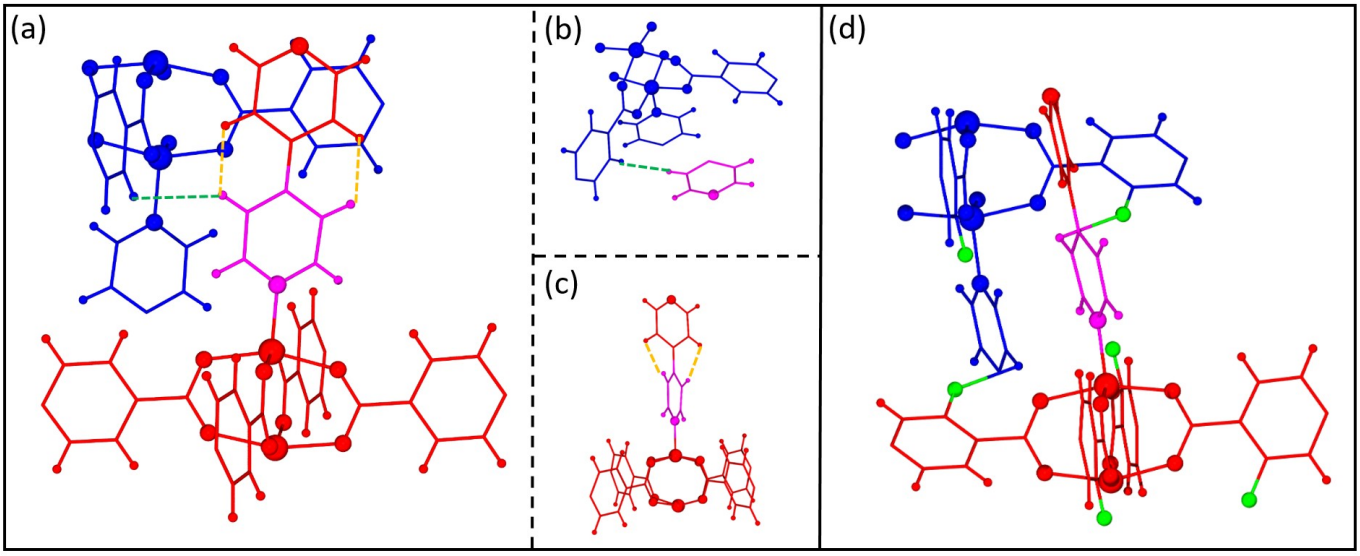

Figure 1. (a) Fragment of LMOF-236 showing the interaction between the two frameworks (red and blue) around a highlighted pyridyl moiety (pink) with significant rotational freedom. The dotted green line shows the closest interaction between the highlighted pyridine and the neighbouring framework (3.8 Å), while the dotted orange lines indicate the closest intramolecular interaction of the bpy via the two H atoms located at the two pyridyl rings (red and pink) of the same framework. (b) Isolated view of the H···H interaction between the highlighted pyridine (pink) and the neighbouring framework. (c) Isolated view of the intramolecular H···H interaction between the two pyridyl groups of bpy (pink and red) within the same framework. (d) Fragment of LMOF-301 showing the interaction between the two frameworks (red and blue)

around a highlighted pyridyl moiety (pink), with the H-F interaction (2.54 Å) shown as a bond between the fluorine atom (green) and the pyridyl hydrogen on the neighbouring framework. All distances given are measured between atom centers.

free H_4tcbpe ligand's quantum yield of 62.3% under the same excitation conditions (table S2).[11]

In both cases, the trends in luminescent efficiency are consistent with our understanding of the LMOFs' structures. In the case of LMOF-301, strong interaction between the fluorine located on the chromophore ligand and the hydrogen located on the bpy ligand serves to rigidify the structure in the absence of pore solvent, which helps to maintain the activated structure's quantum yield. In the case of LMOF-236, the ability of the bpy pyridyl ring to freely rotate in the absence of pore solvent induces a significant drop in the activated structure's quantum yield.

In order to assess how effectively the rotation of the bpy pyridyl moiety could be suppressed, solvent exchange was performed on both LMOF-236 and LMOF-301 with a variety of solvents. Solvents were selected to represent a diverse group of functionalities, molecule size, and molecule shape. Following activation and solvent exchange, quantum yield measurements were taken, and PXRD was used to confirm that the samples remained crystalline. The results are summarized in Table 2.

For LMOF-301, aliphatic solvents had little impact on the quantum yield, indicating that any electronic interactions between the solvent and the LMOF were limited, and that any changes in the general rigidity of the framework itself had no appreciable effect on the quantum yield. Aromatic solvents significantly decreased quantum yield, which may be due to an electronic interaction between the solvent molecules and the LMOF framework.[21] For LMOF-263, quantum yield was significantly decreased upon activation where DMA solvent molecules were removed from the LMOF pores. Upon solvent exchange, quantum yield was significantly increased for both aliphatic and aromatic species, indicating that the presence/inclusion of any solvent molecule was sufficient to restrict the rotation of the bpy pyridyl moiety at different extent. The quantum yields in the presence of aromatic solvents was in trend with those of LMOF-301, and it is possible that these solvents effectively deactivated the pyridyl rotation, but that the same electronic interaction observed in LMOF-301 limited emission. The only solvent to significantly improve on the as-made quantum yield in LMOF-236 was n-pentane, which lifted the quantum yield to 59.3%.

Comparing the PXRD patterns of the pentane-loaded LMOF-263 and LMOF-301 with the activated and simulated patterns,

Table 2. Quantum yields of samples of LMOF-236 and LMOF-301 following solvent exchange under 455 nm excitation

Solvent	QY (LMOF-236)	QY (LMOF-301)
Dimethylacetamide	42.5 % (as made)	50.9 % (as made)
Activated	12.2 %	45.1 %
Acetone	Not stable	Not tested
Ethanol	Not stable	Not tested
Isopropanol	Not stable	Not tested
Glycerol	Not stable	Not tested
Triethylamine	Not stable	Not tested
Dichloromethane	Not stable	Not tested
Ethyl Acetate	27.3 %	49.3 %
N-Pentane	59.3 %	48.5 %
Cyclohexane	44.2 %	44.9 %
Dodecane	43.7 %	41.6 %
Benzene	32.5 %	28.2 %
Toluene	21.7 %	16.7 %

it is apparent that framework flexibility allows both LMOFs to expand upon solvation with n-pentane (Fig. 3).

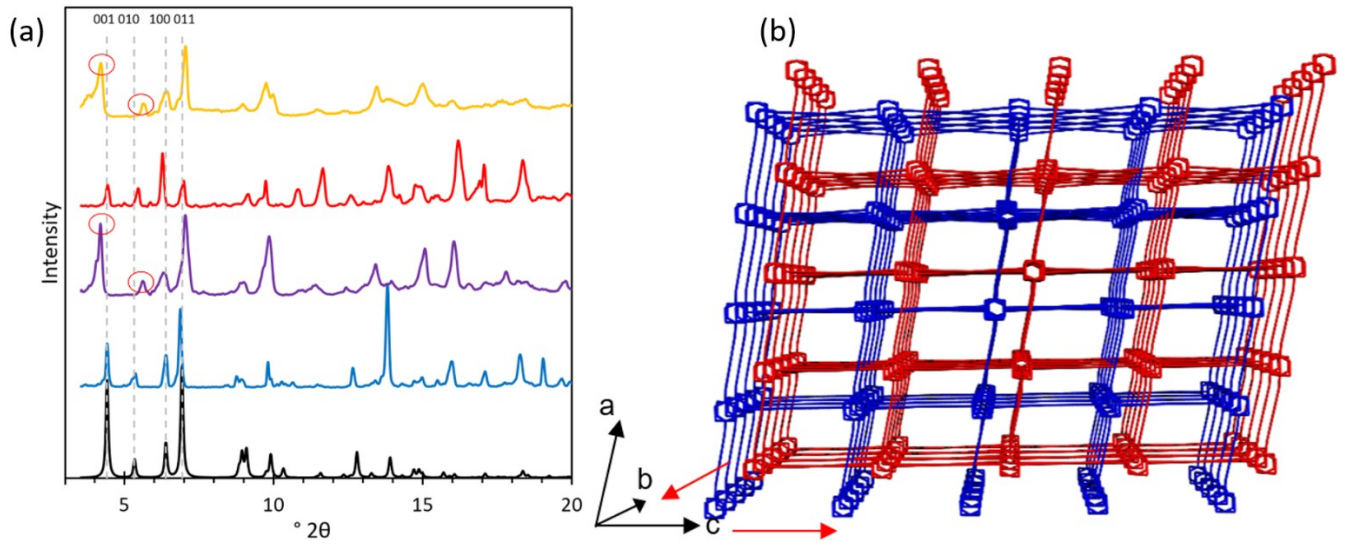

Figure 32. (a) Simulated PXRD pattern of LMOF-263 (black), overlaid with the PXRDs of the activated LMOF-263 (blue), activated LMOF-301 (red), the pentane-loaded LMOF-263 (purple), and pentane-loaded LMOF-301LMOF-301 (gold). The first four peaks are indexed, and the peak changes observed in the pentane-loaded samples are marked with red circles. As LMOF-263 and LMOF-301 are isoreticular with nearly identical unit cells, only the simulated pattern for LMOF-263 is shown. (b) A crystallographic shift that could be responsible for the expansion along the c axis and contraction along the b axis observed in the pentane-loaded samples.

In both pentane-loaded LMOFs, the 001 peak shifts to a lower angle, corresponding to an expansion along the *c* axis (20.01 Å) of 0.95 Å in LMOF-263 and 1.01 Å in LMOF-301, respectively. Simultaneously, the 010 peak shifts to a higher angle, corresponding to a contraction along the *b* axis (16.55 Å) of 0.83 Å for LMOF-263 and 0.87 Å for LMOF-301. This combination of expansion in the *c* direction and contraction in the *b* direction is consistent with a shifting in the relative positon of the two interpenetrated frameworks, which has been previously observed in interpenetrated MOFs.[30, 31] With the frameworks sliding in the negative *b*/positive *c* direction, it would bring LMOF-263's free-rotating pyridyl moiety from one framework nearly into contact with the tcbpe ligand in the other framework, as the nucleus-nucleus H · · · H distance would shrink to just 2.0 Å, effectively rigidifying the ligands.

Conclusions

Developing strategies for the post-synthetic rigidification of LMOFs provides another useful tool to fine-tune and enhance their luminescence. In this report, two isoreticular LMOFs having very similar structure but different framework rigidity are selected as ideal test materials to examine the solvent-packing effect to rigidification. LMOF-236 emission is severely weakened because of a freely-rotating pyridyl ring on the bpy ligand, while LMOF-301 shows very limited flexibility-related emission quenching due to limited rotation of the same pyridyl ring as a result of strong inter-framework hydrogen-fluorine interaction. The structural similarities were discussed, and the structural basis for their divergent behavior was elucidated. Solvents with various functional groups and of various shapes and sizes were loaded into the two LMOFs, and n-pentane was able to enhance the emission from LMOF-236 by 40% with respect to the as-made sample and 386% with respect to the activated sample. Changes in the unit cells of their crystal structures demonstrate that n-pentane shifts the interpenetrated nets in both LMOF-263 and LMOF-301. In LMOF-263, this pushes the freely-rotating pyridyl ring from one net closer to the second net, restricting rotation and restoring emission intensity from the material, while in LMOF-301, the rotation of the pyridyl ring was already restricted, so the same shift does not result in noticeable changes in luminescent efficiency.

Conflicts of interest

There are no conflicts to declare.

Acknowledgements

WPL and JL acknowledge the financial support from the National Science Foundation (Grant No. DMR-1507210). This research used resources of the Advanced Light Source, which is a DOE Office of Science User Facility under contract no. DE-AC02-05CH11231.

References

1. Z. Hu, B. J. Deibert and J. Li, *Chemical Society Reviews*, 2014, **43**, 5815-5840.
2. W. P. Lustig, S. Mukherjee, N. D. Rudd, A. V. Desai, J. Li and S. K. Ghosh, *Chemical Society Reviews*, 2017, **46**, 3242-3285.
3. M. D. Allendorf, C. A. Bauer, R. K. Bhakta and R. J. T. Houk, *Chemical Society Reviews*, 2009, **38**, 1330-1352.

4. Y. Cui, Y. Yue, G. Qian and B. Chen, *Chemical Reviews*, 2012, **112**, 1126-1162.
5. T. N. Nguyen, F. M. Ebrahim and K. C. Stylianou, *Coordination Chemistry Reviews*, 2018, **377**, 259-306.
6. M.-L. Han, G.-X. Wen, W.-W. Dong, Z.-H. Zhou, Y.-P. Wu, J. Zhao, D.-S. Li, L.-F. Ma and X. Bu, *Journal of Materials Chemistry C*, 2017, **5**, 8469-8474.
7. R.-W. Huang, Y.-S. Wei, X.-Y. Dong, X.-H. Wu, C.-X. Du, S.-Q. Zang and T. C. W. Mak, *Nature Chemistry*, 2017, **9**, 689.
8. S. Mollick, T. N. Mandal, A. Jana, S. Fajal, A. V. Desai and S. K. Ghosh, *ACS Applied Nano Materials*, 2019, **2**, 1333-1340.
9. T. Kundu, S. Mitra, D. Díaz Díaz and R. Banerjee, *ChemPlusChem*, 2016, **81**, 728-732.
10. W. P. Lustig and J. Li, *Coordination Chemistry Reviews*, 2018, **373**, 116-147.
11. Z. Hu, G. Huang, W. P. Lustig, F. Wang, H. Wang, S. J. Teat, D. Banerjee, D. Zhang and J. Li, *Chemical Communications*, 2015, **51**, 3045-3048.
12. Q. Gong, Z. Hu, B. J. Deibert, T. J. Emge, S. J. Teat, D. Banerjee, B. Mussman, N. D. Rudd and J. Li, *Journal of the American Chemical Society*, 2014, **136**, 16724-16727.
13. B. J. Deibert, E. Velasco, W. Liu, S. J. Teat, W. P. Lustig and J. Li, *Crystal Growth & Design*, 2016, **16**, 4178-4182.
14. Z. Wei, Z.-Y. Gu, R. K. Arvapally, Y.-P. Chen, R. N. McDougald, J. F. Ivy, A. A. Yakovenko, D. Feng, M. A. Omary and H.-C. Zhou, *Journal of the American Chemical Society*, 2014, **136**, 8269-8276.
15. J.-x. Ma, X.-f. Huang, X.-q. Song and W.-s. Liu, *Chemistry – A European Journal*, 2013, **19**, 3590-3595.
16. M. Zhang, G. Feng, Z. Song, Y.-P. Zhou, H.-Y. Chao, D. Yuan, T. T. Y. Tan, Z. Guo, Z. Hu, B. Z. Tang, B. Liu and D. Zhao, *Journal of the American Chemical Society*, 2014, **136**, 7241-7244.
17. N. B. Shustova, A. F. Cozzolino, S. Reineke, M. Baldo and M. Dincă, *Journal of the American Chemical Society*, 2013, **135**, 13326-13329.
18. B. Jousselme, P. Blanchard, P. Frère and J. Roncali, *Tetrahedron Letters*, 2000, **41**, 5057-5061.
19. K. Pyo, V. D. Thanthirige, K. Kwak, P. Pandurangan, G. Ramakrishna and D. Lee, *Journal of the American Chemical Society*, 2015, **137**, 8244-8250.
20. J. A. Jacobsen, J. R. Stork, D. Magde and S. M. Cohen, *Dalton Transactions*, 2010, **39**, 957-962.
21. F. Wang, W. Liu, S. J. Teat, F. Xu, H. Wang, X. Wang, L. An and J. Li, *Chemical Communications*, 2016, **52**, 10249-10252.
22. A. D. Becke, *Physical Review A*, 1988, **38**, 3098-3100.
23. C. Lee, W. Yang and R. G. Parr, *Physical Review B*, 1988, **37**, 785-789.
24. C. Sosa, J. Andzelm, B. C. Elkin, E. Wimmer, K. D. Dobbs and D. A. Dixon, *The Journal of Physical Chemistry*, 1992, **96**, 6630-6636.
25. A. D. Becke, *The Journal of Chemical Physics*, 1993, **98**, 1372-1377.
26. M. J. Frisch, J. A. Pople and J. S. Binkley, *The Journal of Chemical Physics*, 1984, **80**, 3265-3269.
27. F. Grein, *The Journal of Physical Chemistry A*, 2002, **106**, 3823-3827.
28. D. O'Reilly, R. S. Stein, M. B. Patrascu, S. K. Jana, J. Kurian, N. Moitessier and M. J. Damha, *Chemistry – A European Journal*, 2018, **24**, 16432-16439.
29. W. P. Lustig, F. Wang, S. J. Teat, Z. Hu, Q. Gong and J. Li, *Inorganic Chemistry*, 2016, **55**, 7250-7256.
30. K. L. Mulfort, O. K. Farha, C. D. Malliakas, M. G. Kanatzidis and J. T. Hupp, *Chemistry – A European Journal*, 2010, **16**, 276-281.

31. Y.-S. Bae, D. Dubbeldam, A. Nelson, K. S. Walton, J. T. Hupp and R. Q. Snurr, *Chemistry of Materials*, 2009, **21**, 4768-4777.